

Spectroscopic characterisation of $\text{LaGaO}_3:\text{Er}^{3+}$ crystals

I. Sokólska^{1,2}

¹ Institut für Laser-Physik, Universität Hamburg, Jungiusstraße 9a, 20355 Hamburg, Germany
(E-mail: sokolska@physnet.uni-hamburg.de)

² W. Trzebiatowski Institute of Low Temperature and Structure Research, Polish Academy of Sciences, 50-950 Wrocław, P.O. Box 1410, Poland

Received: 6 December 1999/Revised version: 10 February 2000/Published online: 27 April 2000 – © Springer-Verlag 2000

Abstract. LaGaO_3 crystals doped with Er^{3+} ions were grown by the Czochralski method and their optical properties were examined. The Er^{3+} energy levels have been determined from the low-temperature absorption and emission spectra. The results of Judd–Ofelt analysis are presented and compared with experimental data. The emission cross sections are determined for the ${}^4I_{13/2} \rightarrow {}^4I_{15/2}$ (1.55 μm) and ${}^4I_{11/2} \rightarrow {}^4I_{13/2}$ (2.85 μm) transitions of erbium.

PACS: 42.70.Hj; 78.20 -e; 78.55-

Lanthanum orthogallate LaGaO_3 belongs to the wide group of the compounds of general ABO_3 formula (A – rare earth ion, B – Al, Ga, Fe, Cr, V) and crystallise in a distorted perovskite structure [1]. At room temperature (RT) the crystal belongs to the centrosymmetric space group $Pbnm$ (orthorhombic) but at higher temperatures undergoes phase transitions. At temperature of about 145 °C the first-order phase transition accompanied by a structural transformation to the rhombohedral group $R3c$ takes place [2, 3]. At temperature of about 1180 °C a second-order transition without structural changes was detected [3]. The existence of phase transitions is a main obstacle to grow crystals of a good optical quality, as they tend to become twinned [3, 4]. The first LaGaO_3 crystals investigated were grown by a solid state reaction [5] or from a flux [6]. However, after stating their very good lattice and thermal expansion matching to the high- T_c -superconducting $\text{YBa}_2\text{Cu}_3\text{O}_7$ (YBCO) films [7], the technology of LaGaO_3 crystal growth has significantly improved. Single crystals grown by the Czochralski method are nowadays commonly used as substrates for the growth of superconducting films [2–4, 8].

From the point of view of optical applications LaGaO_3 is also an interesting host, as it allows substitution in the La^{3+} site by rare-earth (RE) luminescent/laser ions or in the distorted octahedral Ga^{3+} site by transition-metal ions. Recently, spectroscopic properties of LaGaO_3 crystals doped with neodymium [9], chromium [10], vanadium and cobalt [11] have been investigated. In this paper optical properties of erbium-doped LaGaO_3 are presented. Er-doped materials are still of interest because of the growing application range for mid- and far-infrared lasers, based so far mainly on Er^{3+} ,

Ho^{3+} , and Tm^{3+} ions. Hence many oxide crystals (among others YAG [12], YAlO_3 [12, 13], YVO_4 [14], Y_2SiO_5 [15]) as well as fluoride crystals (for example LaF_3 , LiYF_4 [12, 13]) and glasses [16] have been investigated in detail with a special interest put on the transitions around 1.55 μm (${}^4I_{13/2} \rightarrow {}^4I_{15/2}$) and 2.8 μm (${}^4I_{11/2} \rightarrow {}^4I_{13/2}$). The results obtained for erbium-doped LaGaO_3 in this work are compared with those for some other Er^{3+} -doped materials.

1 Crystal growth and experimental

$\text{LaGaO}_3:\text{Er}^{3+}$ crystals investigated were grown by the Czochralski method in a nitrogen atmosphere from a stoichiometric mixture of La_2O_3 , Ga_2O_3 , and Er_2O_3 oxides. The Er^{3+} concentration in the melt was 0.8%, 2.8%, and 4%. In order to obtain crystals with minimised density of twins and of a good optical quality, oriented seeds were used ((100) direction) for growth [4]. However, despite this, the optical quality of obtained crystals was not satisfactory. The best quality was obtained for the lowest doped crystal, which was transparent with some traces of micro-twins, mainly along the growth direction. The higher doped crystals were partially milky, containing large amounts of micro-twins and possibly also of nonstoichiometric inclusions. The erbium concentration obtained from the microprobe analysis was about 0.25 at %, 0.3 at %, and 0.5 at % respectively. Taking into account the results obtained for the transparent, low-doped crystal, the segregation coefficient k for Er^{3+} in LaGaO_3 is about 0.3. All Er^{3+} -doped LaGaO_3 crystals investigated were orange, similar in colour to the undoped crystal probably due to large amounts of crystal host defects [3].

The absorption spectra were measured with a 2400 Cary (Varian) spectrophotometer. Luminescence spectra and lifetimes were measured after excitation with an optical parametric oscillator (OPO, Continuum, 7 ns pulse, 10 Hz) or by frequency-doubled Nd:YVO₄ (Millenia, 200 mW, CW 531 nm line) in a typical set-up consisting of a GDM 1-m or a SPEX 0.5-m grating monochromator, a cooled photomultiplier applied for the visible (VIS) range or a Ge diode for the infrared (IR) range, a SRS 250 boxcar integrator or a SRS lock-in amplifier and a personal computer.

The low-temperature (5 K) measurements were performed in a continuous-flow helium cryostat (Oxford CF 1204).

Due to the presence of large amounts of twins and possible other phases the orientation of the samples was not possible and only unpolarised measurements were performed.

2 Results and discussion

In Fig. 1 the room-temperature absorption spectrum of $\text{LaGaO}_3:\text{Er}^{3+}$ is presented. Apart from the typical bands due to the Er^{3+} ($4f^{11}$) intraconfigurational transitions, some strong and broad bands give rise to the absorption for wavelengths shorter than 650 nm. Those bands are probably due to various types of defect centres present in this type of crystal, as they are observed also for undoped crystal (see Fig. 1, inset). The nature of those bands has not been studied in detail yet. Up to now it was stated only that growth conditions, gas atmosphere, and temperature influence the colour of the crystals but the efforts to remove the colour were not successful yet [3]. For the crystals investigated in this work long annealing (ca. 100 h) at 800 °C of both doped and undoped crystals was performed. As is seen from the Fig. 1 (inset), the annealing procedure influences partially the absorption spectra, as the intensity of the absorption band about 500 nm significantly decreases for doped crystals and the crystals become yellow. Similar changes are observed after irradiation of the sample with visible light of a high intensity (OPO, 531 nm line of doubled $\text{Nd}:\text{YVO}_4$). The systematical study of those defects could be performed in order to improve the growth technology of these crystals but was not the goal of the present work.

From the absorption measurements performed at low temperature it was possible to determine the position of Er^{3+} energy levels up to the ${}^4F_{7/2}$ multiplet (Table 1). Higher lying Er^{3+} bands are overlapped by much stronger bands due to defects and could not be determined precisely. The number of Stark split components at low temperature is for all observed transitions consistent with the expected number of $(2J + 1)/2$.

Table 1. Energy of Stark levels of Er^{3+} multiplets in LaGaO_3 crystal, overall splittings of the multiplets and oscillator strengths due to the electric-dipole transitions from the ground ${}^4I_{15/2}$ to the higher multiplets. Experimental oscillator strengths f_{exp} were determined from the absorption spectrum, calculated values were obtained from a standard Judd-Ofelt analysis

Er^{3+} multiplet	Energy levels/ cm^{-1}	Overall splitting/ cm^{-1}	Experimental oscillator strength $f_{\text{exp}} \times 10^{-6}$	Calculated oscillator strength $f_{\text{calc}} (\text{ed}) \times 10^{-6}$
${}^4F_{7/2}$	20 479, 20 536, 20 587, 20 648	169	2.20	2.00
${}^2H_{11/2}$	19 124, 19 150, 19 177, 19 205, 19 251, 19 270	146	10.81	10.80
${}^4S_{3/2}$	18 422, 18 479	57	0.53	0.39
${}^4F_{9/2}$	15 266, 15 334, 15 375, 15 390, 15 421	155	3.81	3.84
${}^4I_{9/2}$	12 395, 12 425, 12 592, 12 609, 12 678	203	0.80	0.72
${}^4I_{11/2}$	10 265, 10 277, 10 298, 10 320, 10 346, 10 358	93	0.50	0.43
${}^4I_{13/2}$	6 581, 6 622, 6 654, 6 677, 6 732, 6 749, 6 795	214	1.64 (ed+md) 0.99 (ed) 0.65 (md)*	1.037 (ed)
${}^4I_{15/2}$	0, 38, 161, 191, 212, 322, 350, 437	437		

* the contribution of magnetic-dipole component was calculated according to (3)

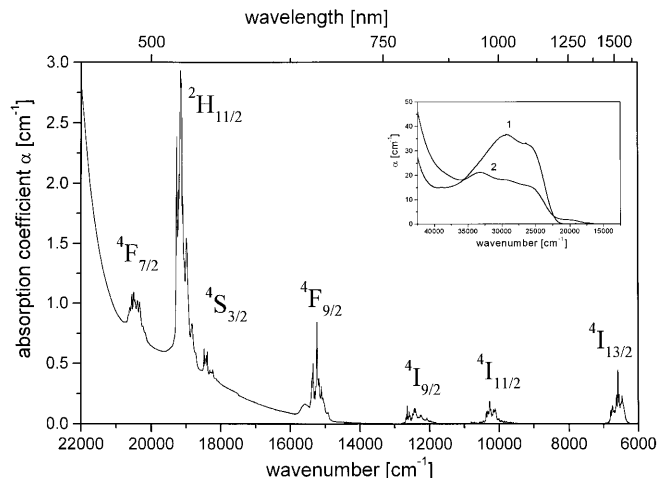


Fig. 1. Absorption spectrum of a $\text{LaGaO}_3:\text{Er}^{3+}$ crystal (0.3 at %) recorded at RT. In the inset the absorption spectra of a $\text{LaGaO}_3:\text{Er}^{3+}$ crystal annealed 100 h at 800 °C (curve 1) and undoped LaGaO_3 “as received” crystal (curve 2) are presented

Er^{3+} -doped LaGaO_3 crystals exhibit typical Er^{3+} luminescence from ${}^4S_{3/2}$, ${}^4F_{9/2}$, ${}^4I_{11/2}$, and ${}^4I_{13/2}$ multiplets (Fig. 2) as well as green “up-converted” luminescence from ${}^4S_{3/2}$ multiplet. The low-temperature spectra of luminescence terminating at the ground ${}^4I_{15/2}$ state permit us to determine the position of its Stark components. As an example, in Fig. 3 the well-resolved eight components due to the ${}^4S_{3/2} \rightarrow {}^4I_{15/2}$ transition are presented.

The lifetimes of main erbium multiplets measured at RT and 5 K are listed in Table 2. In the investigated range of relatively low Er^{3+} concentrations, its effect on the lifetime is not pronounced and one can assume the negligible contribution of the concentration quenching processes on the transition rate. The uncertainty of the lifetime values measured for the ${}^4I_{13/2} \rightarrow {}^4I_{15/2}$ transition is determined by the experimental conditions and by the radiation trapping effect which tends to lengthen the experimentally measured lifetime, see for example [17]. The values listed in Table 2 have been obtained after the resonant excitation of pertinent levels with the OPO.

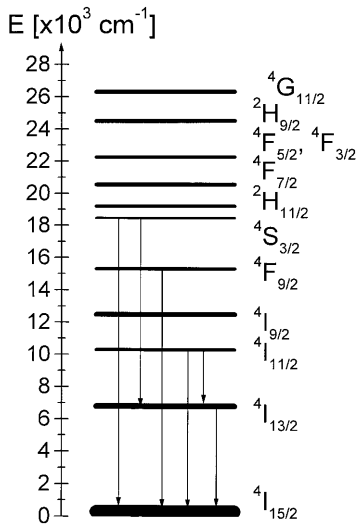


Fig. 2. Energy level scheme and main luminescent transitions of Er^{3+} ion in LaGaO_3 crystal

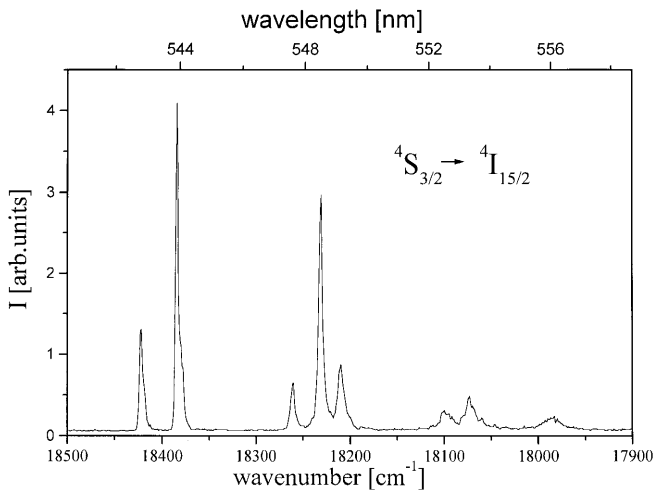


Fig. 3. Luminescence spectrum of $\text{LaGaO}_3:\text{Er}^{3+}$ (0.3 at %) due to the ${}^4S_{3/2} \rightarrow {}^4I_{15/2}$ transition recorded at 5 K

The emission from the ${}^4I_{13/2}$ level is much stronger when exciting the ${}^4I_{11/2}$ level. The ${}^4I_{13/2}$ decay curves in this case are presented in Fig. 4 for all crystals investigated. The curves can be fitted with a good accuracy by the following equation

$$I(t) = A e^{-t/\tau_1} - B e^{-t/\tau_2}, \quad (1)$$

which is the solution of rate equations connecting three involved levels ${}^4I_{11/2}$, ${}^4I_{13/2}$, and ${}^4I_{15/2}$, where A , B are parameters, τ_1 and τ_2 are the lifetimes (inverse of transition rates) from ${}^4I_{13/2}$ and ${}^4I_{11/2}$ levels, respectively. The values of τ_1 and τ_2 obtained from the fit are given in Fig. 4 and are in agreement with values obtained after resonant excitation within the accuracy of fit and experiment.

As the concentration does not influence the lifetime of any level, we can assume that the decay is governed mainly by radiative transition and multiphonon relaxation. For Er^{3+} doped materials the method based on the Judd–Ofelt (J–O) theory [18, 19] is often used to determine the contribution of radiative transitions to the excitation decay and gives relatively

Table 2. Lifetime of the Er^{3+} main multiplets in LaGaO_3 crystals investigated

Multiplet	0.25% at		0.3% at		0.5% at	
	300 K		300 K		5 K	
${}^4S_{3/2}$	270 μs	260 μs	230 μs	350 μs		
${}^4F_{9/2}$	100 μs	95 μs	95 μs	105 μs		
${}^4I_{11/2}$	3.0 ms	2.8 ms	2.95 ms	3.3 ms		
${}^4I_{13/2}$	–	4.2–4.4 ms	4.5–4.65 ms	4.5 ms		

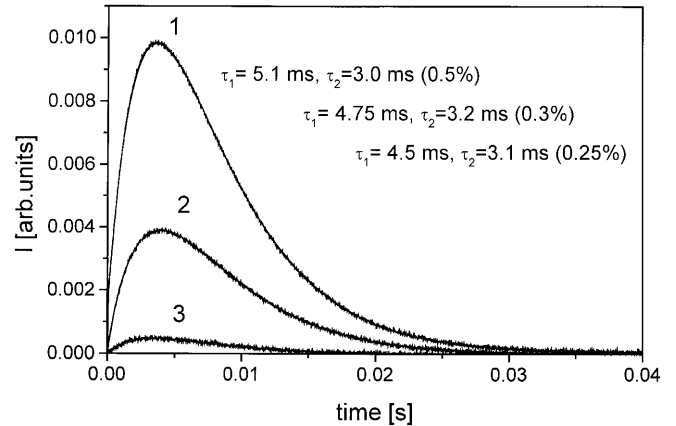


Fig. 4. Luminescence decay curves for ${}^4I_{13/2}$ multiplet recorded at RT after excitation of ${}^4I_{11/2}$ multiplet (OPO, $\lambda_{\text{exc}} \approx 972$ nm) for $\text{LaGaO}_3:\text{Er}^{3+}$ crystals with dopant concentration: 1 – 0.5 at %, 2 – 0.3 at %, 3 – 0.25 at %

good agreement with experimental data, for example [20–22]. According to the J–O theory, the oscillator strength for an electric-dipole transition between states $4f^n[L, S]J$ and $4f^n[L', S']J'$, respectively, is expressed as follows

$$f_{\text{ed}} = \frac{8\pi^2 mc}{3h\lambda(2J+1)} \frac{(n^2+2)^2}{9n} \times \sum_t \Omega_t \left| \langle 4f^n[L, S]J || U^t || 4f^n[L', S']J' \rangle \right|^2, \quad (2)$$

where λ is the average wavelength of the transition, n is the index of refraction of the material ($n = 2.17$ for LaGaO_3), Ω_t are phenomenological parameters and $\langle || U^t || \rangle$ are the doubly-reduced unit tensor operators calculated for the intermediate coupling case, tabulated for example in [23]. The oscillator strength for a magnetic-dipole transition is given by the equation

$$f_{\text{md}} = \frac{nh}{6mc\lambda(2J+1)} \times \left| \langle 4f^n[L, S]J || L + 2S || 4f^n[L', S']J' \rangle \right|^2, \quad (3)$$

where the matrix element of the magnetic-dipole operator $L + 2S \left| \langle 4f^n[L, S]J || L + 2S || 4f^n[L', S']J' \rangle \right|^2$ are tabulated for main strong transitions of magnetic-dipole character [24] or can be calculated with the formula given in for example [23, 24].

On the other hand, oscillator strengths can be determined experimentally from the absorption spectrum as

$$f_{\text{exp}} = \frac{4\varepsilon_0 m c^2}{N e^2 \lambda_m^2} \int \alpha(\lambda) d\lambda, \quad (4)$$

where ε_0 is a dielectric constant, m and e are the electron mass and charge, respectively, c is the velocity of light, N is the concentration of optically active ions, λ_m is the mean wavelength of the transition and $\int \alpha(\lambda) d\lambda$ is the integrated absorption coefficient. The total oscillator strength is due to electron transitions of electric-dipole as well as magnetic-dipole character $f_{\text{exp}} = f_{\text{ed}} + f_{\text{md}}$, however, in most cases the magnetic-dipole component is of the order 10^{-8} and is negligible comparing with the electric-dipole component ($10^{-6} - 10^{-5}$). In the case of Er^{3+} ions the absorption transition ${}^4I_{15/2} \rightarrow {}^4I_{13/2}$ as well as emission transitions ${}^4I_{13/2} \rightarrow {}^4I_{15/2}$ and ${}^4I_{11/2} \rightarrow {}^4I_{13/2}$ contain significant contribution of magnetic-dipole component which has to be calculated in the J–O approach according to (3). Comparing (4) with (2) and (3) the set of equations for absorption transitions from the ground state to higher multiplets can be constructed, from which three Ω_t parameters can be determined in the fitting procedure. Usually, for Er^{3+} -doped materials a set of about eight up to eleven equations for transitions from the ground ${}^4I_{15/2}$ state to multiplets up to ${}^2G_{7/2}$ can be used and Ω_t parameters are determined with a good accuracy [20–22]. For the material investigated in this work, the set of seven equations only was evaluated, as the oscillator strengths for transitions to the high-lying multiplets could not be obtained from the absorption spectrum. In the fitting procedure the experimentally determined oscillator strengths listed in Table 1 were used.

The obtained Ω_t parameters are: $\Omega_2 = 3.59 \times 10^{-20} \text{ cm}^2$, $\Omega_4 = 2.49 \times 10^{-20} \text{ cm}^2$, and $\Omega_6 = 0.44 \times 10^{-20} \text{ cm}^2$. As a measure of a fit quality, the root mean square (RMS) deviation is often used:

$$\text{RMS} - \Delta f = \left(\frac{\sum (\Delta f_i)^2}{M - 3} \right)^{1/2}, \quad (5)$$

where Δf_i are the residuals between the experimental (f_{exp}) and calculated (f_{calc}) oscillator strengths, M is the number of equations. In spite of a relatively low number of transitions taken into account for calculation, the RMS deviation

in the case of $\text{LaGaO}_3:\text{Er}^{3+}$ is equal to 16.8×10^{-8} , being comparable with values obtained for other hosts, see for example [17, 20, 21].

The Ω_t parameters were used further to calculate the radiative rates of the electric-dipole transitions from luminescent multiplets to lower states according to the formula

$$A_{\text{ed}} = \frac{16\pi^3 e^2 n(n^2 + 2)^2}{27h\varepsilon_0 \lambda^3 (2J + 1)} \times \sum_{t=2,4,6} \Omega_t \left| \left\langle 4f^n [L, S] J \left\| U^t \right\| \left\langle 4f^n [L', S'] J' \right\rangle \right|^2. \quad (6)$$

In the case of transitions containing both electric and magnetic components transition rates of magnetic-dipole character were calculated as

$$A_{\text{md}} = \frac{2\pi n^2 e^2}{\varepsilon_0 m c \lambda^2} \times f_{\text{md}}, \quad (7)$$

where f_{md} is given by (3). The transition rates A_{ed} , A_{md} , branching ratios ($\beta_{i \rightarrow j} = A_{i \rightarrow j} / \sum_j A_{i \rightarrow j}$) and calculated radiative lifetime ($1 / \sum_j A_{i \rightarrow j}$) for main Er^{3+} multiplets are summarised in Table 3. The values of calculated radiative lifetime of the ${}^4I_{13/2}$ multiplet are in good agreement with the measured lifetime, taking into account that discrepancies of up to 20% – 30% can be easily introduced both experimentally and by the accuracy of the J–O approach. Whereas for the ${}^4I_{13/2} \rightarrow {}^4I_{15/2}$ transition the contribution of the nonradiative processes should be negligible, from higher multiplets i.e. from ${}^4I_{11/2}$, ${}^4F_{9/2}$, and ${}^4S_{3/2}$ nonradiative transitions are of a certain importance and the measured lifetimes can be much lower than calculated. To estimate the reliability of obtained nonradiative transition rates one can apply the empirical “exponential energy-gap law” [25]

$$w_{\text{nr}} = C e^{-\alpha \Delta E}, \quad (8)$$

where the nonradiative transition rate is determined as $w_{\text{nr}} = \tau_{\text{exp}}^{-1}(5 \text{ K}) - \tau_{\text{calc}}^{-1}$, C and α are constants characteristic of the host, ΔE is the energy gap to the next lower-lying multiplet. The dependence of w_{nr} on the energy gap is presented in Fig. 5. In a logarithmic scale the dependence can be well fitted linearly with $\alpha = 5.3 \times 10^{-3} \text{ cm}^{-1}$, $C = 7.1 \times 10^9 \text{ s}^{-1}$. Those constants are in the range of values obtained for

Table 3. Summary of the results of Judd–Ofelt analysis: calculated branching ratios and radiative lifetimes for main Er^{3+} multiplets in LaGaO_3

Transition between Er^{3+} multiplets	Average wavelength of transition/nm	Branching ratio $\beta_{i \rightarrow j}$	Transition rate/ s^{-1} $A_{\text{ed}, i \rightarrow j}$	Transition rate/ s^{-1} $A_{\text{md}, i \rightarrow j}$	Calculated radiative lifetime of the multiplet/ μs
${}^2H_{11/2} \rightarrow {}^4I_{13/2}$	798	0.021	335		60
	525	0.979	16 365		
${}^4S_{3/2} \rightarrow {}^4I_{9/2}$	1716	0.061	116		530
	1230	0.025	47		
	846	0.266	501		
	545	0.648	1223		
${}^4F_{9/2} \rightarrow {}^4I_{9/2}$	3700	0.001	5.6		209
	2000	0.017	80		
	1150	0.050	240		
	658	0.932	4442		
${}^4I_{11/2} \rightarrow {}^4I_{13/2}$	2700	0.183	27	26	4255
	980	0.817	182		
${}^4I_{13/2} \rightarrow {}^4I_{15/2}$	1536	1	145	92	4219

other hosts ($\alpha \approx 3.5 - 5.5 \times 10^{-3}$, $C \approx 10^8 - 10^{13}$ [17, 21, 25]). The values are similar to those for YAlO_3 crystal ($\alpha = 4.6 \times 10^{-3}$, $C = 5 \times 10^{-9}$ [25]), which has somehow higher maximal host phonon frequencies compared to LaGaO_3 (for Raman phonon analysis of LaGaO_3 , see for example [26]).

In the case of the ${}^4S_{3/2}$ level another additional channel of decay arises at higher temperatures due to thermal occupation of the ${}^2H_{11/2}$ level. The study of temperature dependence of decay kinetics can be performed in the future to examine the contribution of nonradiative processes in this material in more detail. To a certain extent discrepancies between the experimental data and presented results of J–O treatment are due to internal uncertainties of the method, see for example [24] and to experimental errors (determination of concentration and oscillator strengths, influence of radiation trapping effect) but in general the results for $\text{LaGaO}_3:\text{Er}^{3+}$ seem to be reliable and not in contradiction with the experimental data. The good match of nonradiative rates to the “energy-gap law” supports the consistency of the J–O results obtained.

The knowledge of spectroscopic data is needed for the estimation of parameters determining laser applications of materials, that is first of all emission cross sections. For the two Er^{3+} transitions of a special interest for laser purposes, i.e. ${}^4I_{13/2} \rightarrow {}^4I_{15/2}$ (1.55 μm) and ${}^4I_{11/2} \rightarrow {}^4I_{13/2}$ (2.85 μm), emission cross sections can be determined from the spectroscopic data by two commonly applied methods, i.e. by the so-called “reciprocity” method and/or by Füchtbauer–Ladenburg (F–L) method (for a detailed description see for example [13]). For the transition to the ground state ${}^4I_{13/2} \rightarrow {}^4I_{15/2}$ both methods can be applied, for a ${}^4I_{11/2} \rightarrow {}^4I_{13/2}$ transition the F–L method only, as in this case the absorption cross section is not known directly from the absorption measurement.

The “reciprocity” method allows us to determine the emission cross section as a function of wavelength $\sigma_{\text{em}}(\lambda)$ from the known ground-state absorption cross section $\sigma_{\text{abs}}(\lambda)$, assuming that Stark level positions of both multiplets are known:

$$\sigma_{\text{em}}(\lambda) = \sigma_{\text{abs}}(\lambda) \frac{Z_l}{Z_u} \exp\left[\frac{E_{ZL} - \frac{hc}{\lambda}}{k_B T}\right], \quad (9)$$

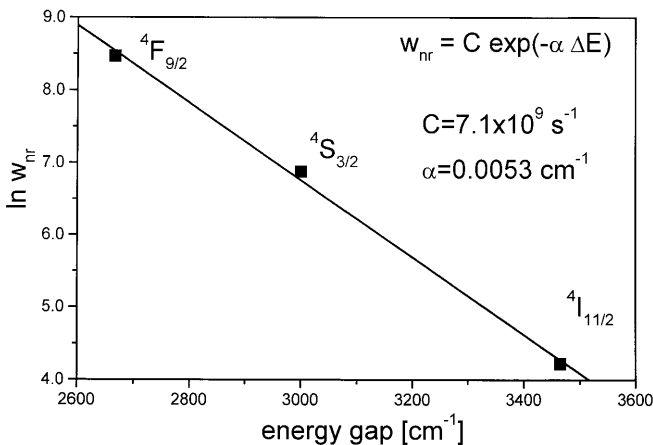


Fig. 5. Dependence of the nonradiative transition rate on the energy gap to the next lower multiplet depicted for ${}^4F_{9/2}$, ${}^4S_{3/2}$, and ${}^4I_{11/2}$ erbium multiplets in LaGaO_3 crystal

where $\sigma_{\text{abs}} = \alpha/N$ is absorption cross section, N – dopant concentration, Z_l , Z_u are partition function of lower (upper) multiplet respectively $Z_l = \sum_i g_i e^{\frac{-E_i}{k_B T}}$, $Z_u = \sum_j g_j e^{\frac{-(E_j - E_{ZL})}{k_B T}}$,

$g_{i,j}$ are degeneracies of the levels, $E_{i,j}$ the energies of Stark levels, E_{ZL} is the energy between the lowest Stark levels of the multiplets involved. The Z_l/Z_u for $\text{LaGaO}_3:\text{Er}^{3+}$ equals 1.24, $E_{ZL} = 6580 \text{ cm}^{-1}$. The maximum value of the emission cross section in the range of about 1550 nm derived according to the above formula equals $9.3 \times 10^{-21} \text{ cm}^2$. The shape of the $\sigma_{\text{em}}(\lambda)$ curve derived by the reciprocity method (Fig. 6, bottom) is in a good accordance with the measured emission spectrum (Fig. 6, top), except for the spectral range where the absorption was too weak to be recorded (above 1600 nm).

From the corrected emission spectrum recorded for the ${}^4I_{13/2} \rightarrow {}^4I_{15/2}$ transition the emission cross sections was derived using the Füchtbauer–Ladenburg formula:

$$\sigma_{\text{em}}(\lambda) = \frac{\lambda^5 I(\lambda)}{8\pi n^2 c \tau_{\text{rad}} \int \lambda I(\lambda) d\lambda}, \quad (10)$$

where $I(\lambda)$ is the intensity of corrected spectrum, τ_{rad} is the radiative lifetime of the ${}^4I_{13/2}$ multiplet obtained from J–O analysis. The emission cross section for 1550 nm derived by this method is $5.9 \times 10^{-21} \text{ cm}^2$. The consistency of results obtained by the above methods is satisfactory. The discrepancy is possibly first of all due to the inaccuracy of the determination of concentration. Comparing the results of the microprobe analysis taken in different regions of the

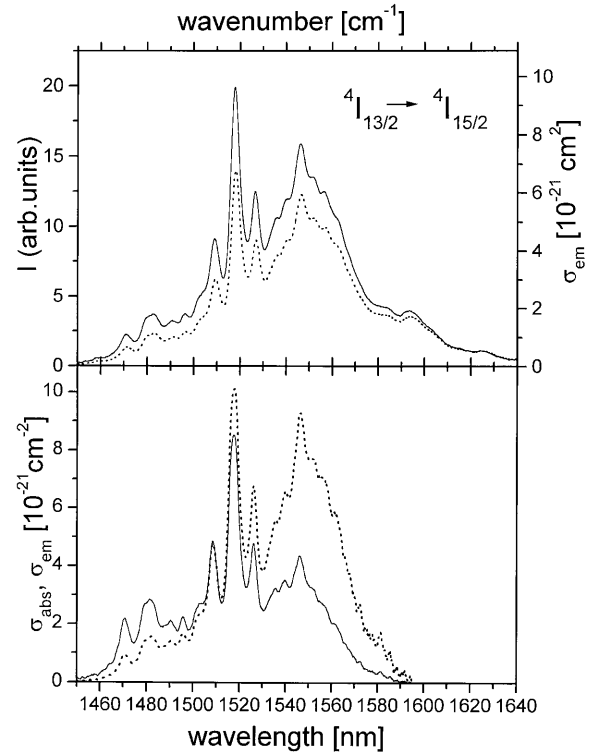


Fig. 6. Emission cross section curves (dotted lines) derived for the ${}^4I_{13/2} \rightarrow {}^4I_{15/2}$ transition around 1.55 μm by the Füchtbauer–Ladenburg method (top layer) from emission spectrum (solid line), and by reciprocity method (bottom layer) from the absorption cross section (solid line)

crystal an error of 25% could be easily introduced (presence of other phases, inhomogeneity of the dopant concentration). Although the lifetime value obtained by the J–O analysis is in an agreement with experimental ones, the actual radiative lifetime could be lower, also contributing to the discrepancy between the above values of emission cross section.

The maximum values of emission cross section obtained for $\text{LaGaO}_3:\text{Er}^{3+}$ for this spectral range are of the typical order or slightly higher than for some other materials investigated (for example σ_{em} at about 1550 nm is $3.1 \times 10^{-21} \text{ cm}^2$ for $\text{YAlO}_3:\text{Er}$ [13], $3.3 \times 10^{-21} \text{ cm}^2$ for $\text{YSO}:\text{Er}$ [15], $4.5 \times 10^{-21} \text{ cm}^2$ for $\text{YAG}:\text{Er}$ [13], $5.5 \times 10^{-21} \text{ cm}^2$ for $\text{YLF}:\text{Er}$ [27]).

The emission cross section for the ${}^4I_{11/2} \rightarrow {}^4I_{13/2}$ transition was derived using the Füchtbauer–Ladenburg formula (Fig. 7). The maximum value of σ_{em} in the spectral range of possible laser oscillation, i.e. for about 2800 nm is about $3 \times 10^{-21} \text{ cm}^2$. This value is somehow lower than estimated for some other materials (for example $4.5 \times 10^{-21} \text{ cm}^2$ for $\text{YAG}:\text{Er}$ [28], $5.7 \times 10^{-21} \text{ cm}^2$ for ZBLAN glass [16], $6.5 \times 10^{-21} \text{ cm}^2$ for $\text{YSGG}:\text{Er}$ [27], $12.5 \times 10^{-21} \text{ cm}^2$ for $\text{YLF}:\text{Er}$ [27]). However, the advantage of LaGaO_3 is the favourable ratio of ${}^4I_{11/2}$ and ${}^4I_{13/2}$ lifetimes (about 1 : 1.3) which could reduce a typical self-terminating behaviour of the 2.85 μm laser transition. This ratio is lower than for many other investigated materials [12, 13] such as YLF (1 : 2.6), BaY_2F_8 (1 : 2.9), YAlO_3 (1 : 80), YAG (1 : 690).

Although the self-terminating could be reduced in a system with a large Stark level splitting (low thermal occupation of higher-lying Stark levels makes the population inversion possible), in most materials investigated so far an additional depopulation path for the ${}^4I_{13/2}$ level is necessary to obtain the free-running laser. In erbium-doped laser materials for this spectral range, usually high doping is applied and efficient up-conversion processes involving the ${}^4I_{13/2}$ multiplet prevent the self-termination. By the favourable lifetimes ratio the need for those additional up-conversion processes can be minimised and laser oscillation could be achieved more easily in such a system.

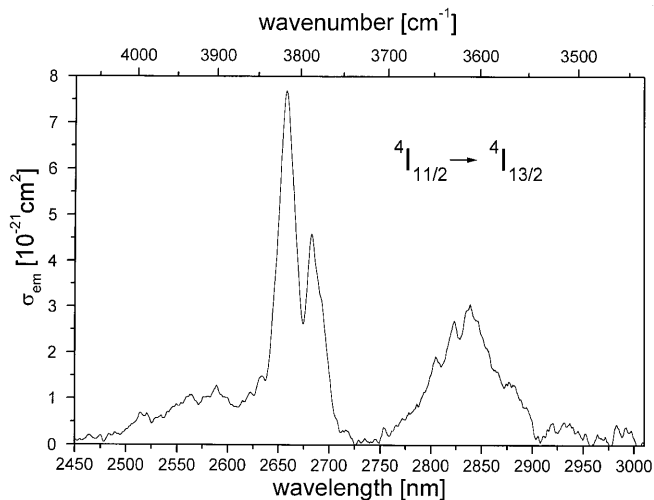


Fig. 7. Emission cross section curve derived for the ${}^4I_{11/2} \rightarrow {}^4I_{13/2}$ transition around 2.8 μm by the Füchtbauer–Ladenburg method

3 Summary

LaGaO_3 crystals doped with Er^{3+} were grown by Czochralski method and their optical properties were investigated. The positions of Stark energy levels were determined from low-temperature spectra. The Judd–Ofelt analysis was performed and the obtained radiative lifetimes are consistent with experimental data. The nonradiative rates estimated for three multiplets follow well the empirical energy-gap law. The emission cross sections estimated for Er^{3+} transitions near 1.55 μm and 2.85 μm are comparable to other materials investigated so far. The advantageous feature of this material for a 2.85 μm laser transition could be a favourable lifetime ratio for involved multiplets. However, for possible practical application the technological problems with growth of good optical quality crystals with higher dopant concentration should be overcome.

Acknowledgements. The author thanks Dr M. Berkowski from the Institute of Physics of the Polish Academy of Science for growing the LaGaO_3 crystals investigated. The author is a holder of the German DFG scholarship in the frame of the Graduierten-Kolleg no.463 at University of Hamburg, where part of this work was done.

References

1. M.L. Keith, R. Roy: *Am. Min* **39**, 1 (1954)
2. W. Marti, P. Fischer, F. Altorfer, H.J. Scheel, M. Tadin: *J. Phys.: Condens. Matter* **6**, 127 (1994)
3. G.W. Berkstresser, A.J. Valentino, C.D. Brandle: *J. Cryst. Growth* **109**, 457 (1991)
4. J. Fink-Finkowicki, M. Berkowski, A. Pajczkowska: *J. Mater. Sci.* **27**, 107 (1992)
5. S. Geller: *Acta Crystallogr.* **10**, 243 (1957)
6. M. Marezio, J.P. Remeika, P.D. Dernier: *Inorg. Chem.* **7**, 1337 (1968)
7. G. Koren, A. Gupta, E.A. Gies, A. Segmuller, R.B. Laibowitz: *Appl. Phys. Lett.* **54**, 1054 (1989)
8. D. Mateika, H. Kohler, H. Laudan, E. Völkel: *J. Cryst. Growth* **109**, 447 (1991)
9. V.M. Orera, L.E. Trinkler, R.I. Merino, A. Larrea: *J. Phys.: Condens. Matter* **7**, 9657 (1995)
10. W. Ryba-Romanowski, S. Golab, G. Dominiak-Dzik, I. Sokółska, M. Berkowski: *J. Alloys Compd.* **284**, 22 (1999)
11. W. Ryba-Romanowski, S. Golab, G. Dominiak-Dzik, M. Berkowski: *J. Alloys Compd.* **288**, 262 (1999)
12. S.A. Payne, L.K. Smith, W.F. Krupke: *J. Appl. Phys.* **77**, 4274 (1995)
13. S.A. Payne, L.L. Chase, L.K. Smith, L. Kway, W.F. Krupke: *IEEE J. Quantum Electron.* **QE-28**, 2619 (1992)
14. F.S. Ermeneux, R. Moncorgé, P. Kabro, J.A. Capobianco, M. Betinelli, E. Cavalli: *OSA Topics on ASSL*, Vol. 1, 498 (1996)
15. C. Li, C. Wyon and R. Moncorgé: *IEEE J. Quantum Electron.* **QE-28**, 1209 (1992)
16. M. Pollnau, C. Ghisler, G. Bunea, W. Lüthy, H.P. Weber: *Appl. Phys. Lett.* **66**, 3564 (1995)
17. J. Amin, B. Dussardier, T. Schweitzer, M. Hempstead: *J. Lumin.* **69**, 17 (1996)
18. B.R. Judd: *Phys. Rev.* **127**, 750 (1962)
19. G.S. Ofelt: *J. Chem. Phys.* **37**, 511 (1962)
20. W. Ryba-Romanowski: *J. Phys. Chem. Solids* **51**, 279 (1990)
21. M.D. Shinn, W.A. Sibley, M.G. Drexhage, R.N. Brown: *Phys. Rev. B* **27**, 6635 (1983)
22. R. Burlot, R. Moncorgé, G. Boulon: *J. Lumin.* **72/74**, 135 (1997)
23. W.T. Carnall, P.R. Fields, K. Rajnak: *J. Chem. Phys.* **49**, 4424 (1968)
24. M.J. Weber: *Phys. Rev.* **157**, 262 (1967)
25. J.M.F. van Dijk, M.F.H. Schuurmans: *J. Chem. Phys.* **78**, 5317 (1983)
26. M.L. Sanjuan, V.M. Orera, R.I. Merino, J. Blasco: *J. Phys.: Condens. Matter* **10**, 11687 (1998)
27. T. Jensen, A. Dening, G. Huber: to be published
28. J. Koetke, G. Huber: *Appl. Phys. B* **61**, 151 (1995)